International Journal of Microwave and Wireless Technologies

cambridge.org/mrf

Gain enhancement of UWB antenna using partially reflective surface

Pravin R. Prajapati and Shailesh B. Khant

Center of Research in Optical, Microwave and Antenna (CROMA) Department of Electronics and Communication Engineering, A D Patel Institute of Technology, Gujarat, India, 388121

Research Paper

Cite this article: Prajapati PR, Khant SB (2018). Gain enhancement of UWB antenna using partially reflective surface. *International Journal of Microwave and Wireless Technologies* **10**, 835–842. https://doi.org/10.1017/S1759078718000326

Received: 16 July 2017
Revised: 7 February 2018
Accepted: 8 February 2018
First published online: 22 March 2018

Keywords:
Antenna design; modelling and measurements; passive components andcircuits

Author for correspondence:
Pravin R. Prajapati,
E-mail: pravinprajapati05@gmail.com

Abstract

This paper proposes, a high gain, Fabry Perot cavity antenna with coplanar waveguide (CPW) fed ultra wide band (UWB) radiating element. The proposed antenna has flat edge arrow shape-based radiating element, which act as a main radiating element and responsible for UWB radiation. This UWB microstrip antenna is parasitically coupled with an array of square parasitic patches (PPs), which act as partially reflective surface. The square patches are fabricated at the bottom of inexpensive FR4 substrate and suspended in the air with the help of dielectric rods at $1.5\lambda_0$ height. High gain is obtained by resonating PPs at near close frequencies of 3.8–8.8 GHz UWB, where partially reflective surface gives almost positive reflection phase gradients. Two laboratory prototypes of antenna, one with and another without partially reflective surface are fabricated and tested. Details of the proposed antenna design and role of partially reflective surface in gain enhancement of planar CPW fed UWB antenna are described, and typical experimental results are presented and discussed.

1. Introduction

Ultra wide band (UWB) communication (3.1–10.6 GHz) [1] is considered as a promising technology for wireless communication systems because of large bandwidth (BW), reduced fading from multi-path, good transmission data-rate and low-power requirements. Antenna is one of the important components, which is responsible for the performance of the UWB communication systems. The recent trends of the development of UWB antennas focus on the development of compact UWB planar antennas because of their simple and low-cost manufacturing process and easily integrating capability with the system board of host devices and lightweight.

The coplanar waveguide (CPW) fed is one of the feeding techniques, which enhances impedance matching for large BW and hence the design of UWB antenna can be realized. In CPW feeding technique, there is no ground on the back side of the planar antenna, which disturbs the radiation at bore-sight, and hence CPW fed UWB antenna suffers from poor gain characteristics [2–5].

Recently, to enhance the gain of the planar antennas, many gain enhancement techniques such as laminated conductor layers [6], parasitic radiation patch [7], by placing a metallic plate as a reflector [8], using microwave lens [9], using array [10], Fabry--Parot cavity [11], Zero index material lens [12], High impedance surface [13], Partially Reflecting Surface (PRS) [14,15], etc. have been reported. In PRS types of structures, the dielectric layer fabricated with parasitic patches (PPs) is placed at approximately 1.5λ distance from the ground plane. This layer has characteristics of partial reflection, so it is known as PRS. These structures are fed by a dipole, microstrip antenna or waveguide. The gain of an antenna with PRS depends on reflection coefficient of PRS, PPs dimension, spacing between PPs, distance between PRS layer and radiating element, etc.

In this paper, an efficient, high gain and ultra wideBW antenna is presented. This paper gives the solution of poor gain characteristics of the CPW fed UWB antenna. With best of our knowledge, in this paper, first time gain enhancement using PRS in the design of CPW fed UWB antenna is reported.

This paper is organized in four sections. In the first section, a brief literature survey of the different gain enhancement techniques, the proposed technique and novelty of the proposed design is presented. In section "Antenna with PRS geometry and its design theory", the description of the CPW fed UWB antenna with PRS geometry and its design theory included. Third section describes experimental results, which contains the comparative results of gain (with and without PRS), the current distribution of PRS and the radiation pattern of the antenna (with and without PRS). The last section covers the conclusion and future work.

CAMBRIDGE UNIVERSITY PRESS

2. Antenna with PRS geometry and its design theory

Figures 1(a) and 1(b) show a top view anda front view of the proposed antenna. The antenna is fed with the CPW technique. The antenna is parasitically coupled with square parasitic patch array (SPPA), which is fabricated from an FR4 superstrate. The complete design dimensions are shown in Table 1.

The array of PPs is known as PRS and it is fabricated on the lower side of the superstrate layer. The superstrate layer is the FR4 substrate with permittivity of 4.4 and loss tangent of 0.018. The parasitic patch dimensions and spacing between them are optimized in order to enhance the gain of the antenna. The length and width of superstrate are $169 \times 169\,\text{mm}^2$ ($4.4\lambda \times 4.4\lambda$ at 7.78 GHz) and thickness is 1.524 mm. Each cell dimension ($d \times d$) are $13 \times 13\tilde{}\text{mm}^2$ ($0.33\lambda \times 0.33\lambda$ at 7.81 GHz), and the spacing or lattice constants of the patches is 14 mm (0.37λ at 7.78 GHz) as shown in Fig. 2. In the proposed structure, the air is act as a dielectric medium between the main radiating element of the antenna and PRS to achieve high efficiency and wide BW. The patch antenna is fed through an SMA jack PCB edge mount RF connector of $50\tilde{}\Omega$. The antenna is designed to operate over 3.8–8.8 GHz of UWB. The superstrate layer is positioned at a height of $1.5\lambda_0$ above the ground plane, where λ_0 is the free-space wavelength corresponding to a central frequency of 7.78 GHz.

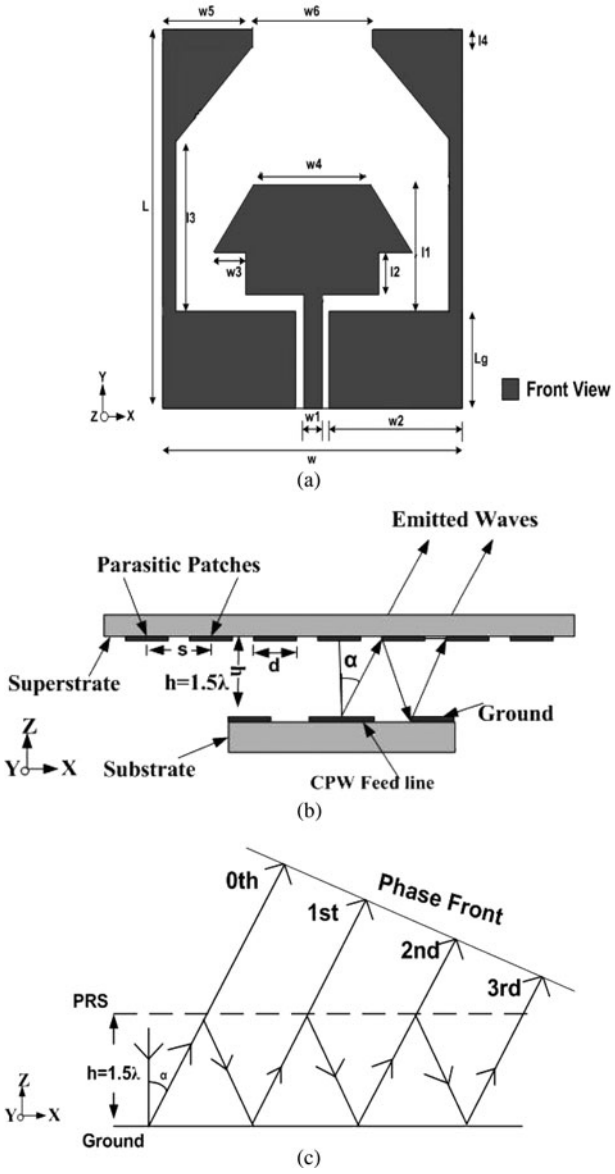

Fig. 1. Design geometry of UWB antenna: (a) top view (in the absence of PRS), (b) front view of the proposed antenna ($d = 13$ mm, $s = 14$ mm, $h = 57.61$ mm), (c) lateral view.

General characteristics of the cavity are, it resonates only at a specific frequency, which results a narrowband resonant antenna. For getting a wideband resonant antenna that maintains the resonance condition over the wide operating frequency band, the reflection phase of the PRS should increase with frequency, as described in [16]. Moreover, every cavity has numerous resonant frequencies that correspond to electromagnetic field modes satisfying necessary boundary conditions on the walls of the cavity. Because of these boundary conditions that must be satisfied with resonance (tangential electric fields must be zero at cavity walls), it follows that cavity length must be an integer multiple of half-wavelength at resonance [17]. In the proposed structure, the CPW fed radiating element and PRS behaves as a cavity and it provides wideband impedance matching (VSWR$\leq$ 2) over the entire ultra wide BW.

In our proposed design, for getting increment in overall reflection phase of the PRS with increment of frequency, the dimensions of the copper cell ($d \times d$), spacing between the adjacent cell, distance between PRS and radiating elements, etc. optimized using CST Microwave Studio simulator V. 2017 [18]. The enhancement of the gain can be explained by partial reflective theory [19–22].

Let the radiation pattern of a UWB source antenna be

$$E_0 \cdot f(\alpha) \tag{1}$$

and for a plane wave, the PRS reflection coefficient (Γ), given by

$$\Gamma = \rho \cdot \exp(j\phi). \tag{2}$$

The magnitude ρ and phase ϕ are generally function of the frequency, the angle of incidence, and the polarization of the emerging electromagnetic wave. An electromagnetic wave radiated by a UWB antenna is not exactly a plane wave when it reaches the PRS. This variation has been neglected in this analysis. To make mathematical analysis simple, PRS is assumed to be lossless here. As shown in Fig. 1 (c), at the phase font, the phase of the referent wave (0th wave) has the relative amplitude of $\sqrt{(1-\rho^2)}$ due to the transmission through the PRS and the successive (1st) wave has the lower relative amplitude of $\rho \cdot \sqrt{(1-\rho^2)}$ due to the one extra reflection from the PRS. This first successive wave is also shifted in phase with respect to the referent wave, due to the

Table 1. Design dimensions of proposed CPW fed UWB antenna with PRS

Parameters	L	W	w_1	w_2	w_3	w_4	w_5	w_6	L_g	l_1	l_2	l_3	l_4
Values (mm)	25	25	3	10.6	2.5	10	7.5	10	8	8.8	3	6.5	1

https://doi.org/10.1017/S1759078718000326 Published online by Cambridge University Press

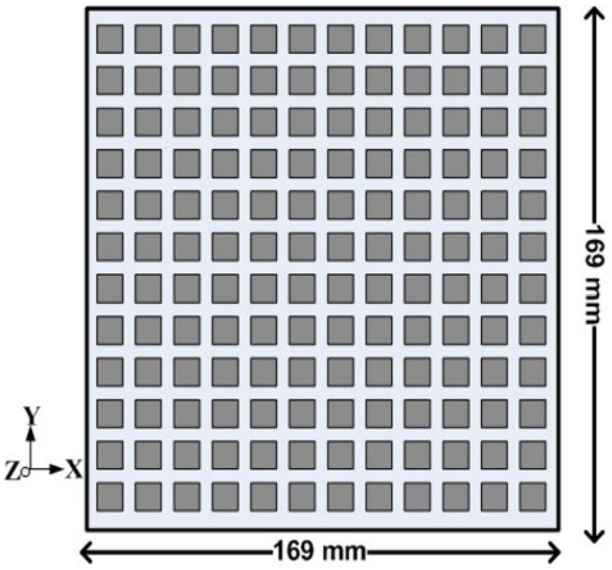

Fig. 2. Design of the proposed PRS.

reflections from the PRS and ground. The phase shift (δ) given by [20,21]:

$$\delta = -\frac{4\pi d}{\lambda} \cdot \cos(\alpha) - \pi + \phi \tag{3}$$

where λ is the free-space wavelength. The first part of equation (3) refers to the difference between the path lengths, $-\pi$ is due to the reflection from the ground plane. For the rest of the successive waves (second, third, etc.) the same theory can be applied, so the relative amplitude and phase of the nth wave in general can be given by

$$\rho^n \cdot \sqrt{(1-\rho^2)}, \tag{4}$$

$$\delta_n = \delta \cdot n = n \cdot (-\frac{4\pi d}{\lambda} \cdot \cos(\alpha) - \pi + \phi), \tag{5}$$

respectively. To achieve the radiation pattern of the PRS antenna, all the waves must be added, and the sum must be modulated by the radiation pattern of the source antenna. It is given by [20,21]

$$E(\alpha) = E_0 \cdot F(\alpha) \cdot \sum_{n=0}^{\infty} \rho^n \cdot \sqrt{(1-\rho^2)} \cdot \exp(jn\delta). \tag{6}$$

The part $\sum_{n=0}^{\infty} \rho^n \cdot \sqrt{(1-\rho^2)} \cdot \exp(jn\delta)$ forms a geometric series. As the PRS is a passive device, the reflection coefficient (Γ) will be <1, and equation (6) can be written as

$$E(\alpha) = E_0 \cdot F(\alpha) \cdot \frac{\sqrt{(1-\rho^2)}}{1-\rho \cdot \exp(j\delta)}. \tag{7}$$

The power pattern given by the standard equation

$$S(\alpha) = \frac{|E(\alpha)|^2}{2\eta} \tag{8}$$

combining equations (7) and (8), the resultant power pattern of

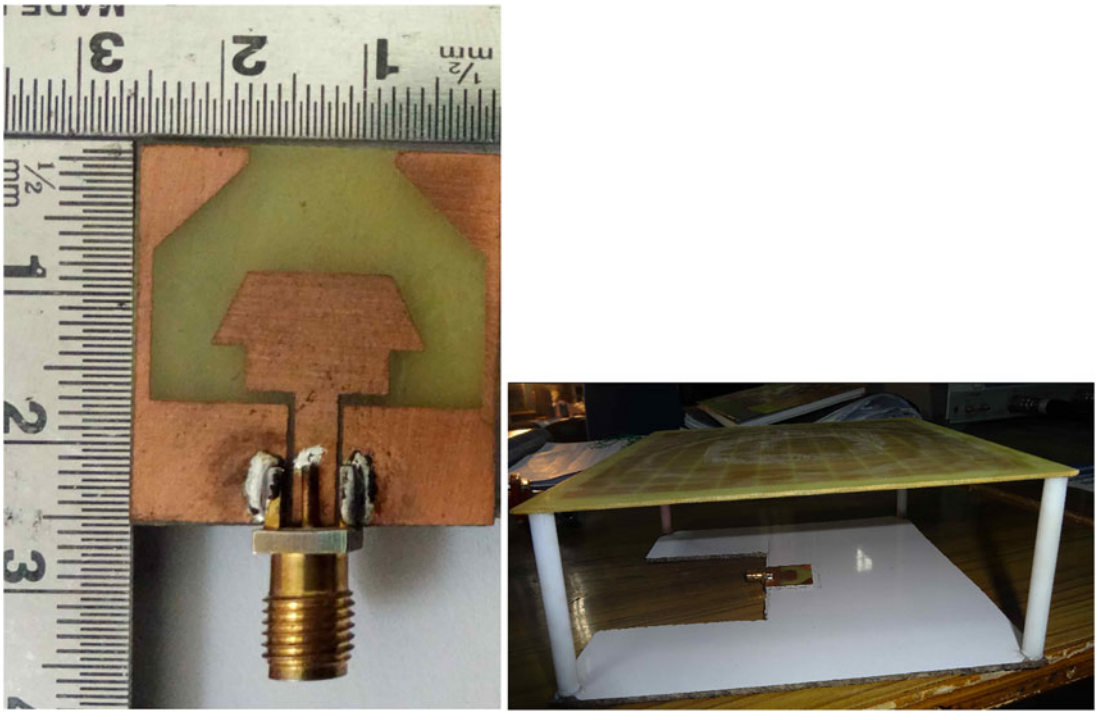

Fig. 3. Fabricated UWB antenna. (a) Top view, (b) antenna with PRS.

https://doi.org/10.1017/S1759078718000326 Published online by Cambridge University Press

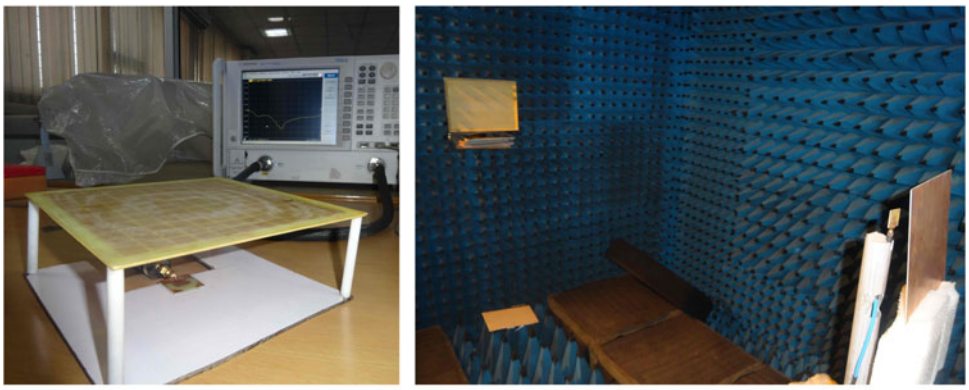

Fig. 4. Measurement setup of proposed antenna (with PRS). (a) Antenna with VNA for BW measurement, (b) antenna at anechoic chamber for measurement of radiation pattern.

the lossless PRS antenna can be obtained, and it is given by

$$S(\alpha) = \frac{|E_0 \cdot F(\alpha)|^2}{2\eta} \cdot \frac{1-\rho^2}{1+\rho^2-2\rho\cdot\cos(\phi-\pi-\frac{4\pi d}{\lambda}\cdot\cos(\alpha))} \quad (9)$$

where η is the intrinsic impedance of free space (120π). The first part of equation (9) is the power pattern of the antenna and the second part gives the value of extra directivityD_e. In other words, the resultant power pattern of the PRS antenna is the power pattern of the source antenna multiplied by the extra directivity.

Maximum power obtained at boresight ($\alpha = 0$) is when the phase condition

$$\phi - \pi - \frac{4\pi d}{\lambda} = 2N\pi, \quad (10)$$

where $N = 0, 1, 2, 3, \ldots$

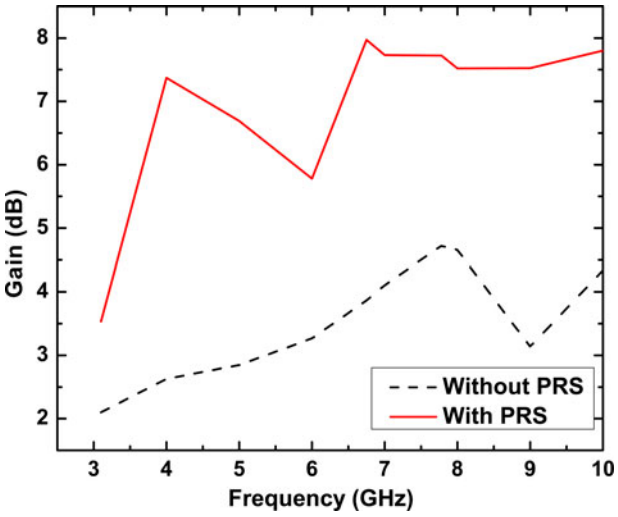

Fig. 6. Simulated gain comparison of antenna (with and without PRS).

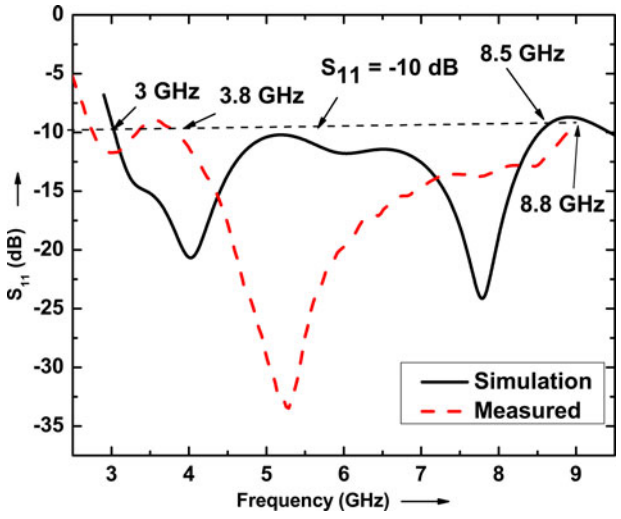

Fig. 5. Comparison of simulated and measured S_{11} of antenna with PRS.

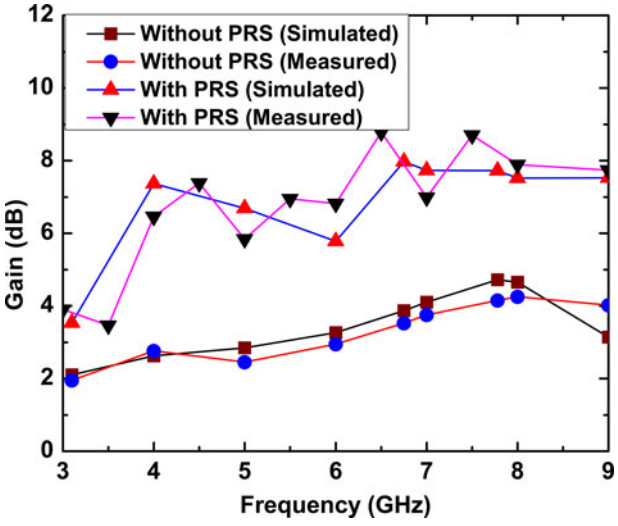

Fig. 7. Simulated and measured gain comparison of antenna (with and without PRS).

https://doi.org/10.1017/S1759078718000326 Published online by Cambridge University Press

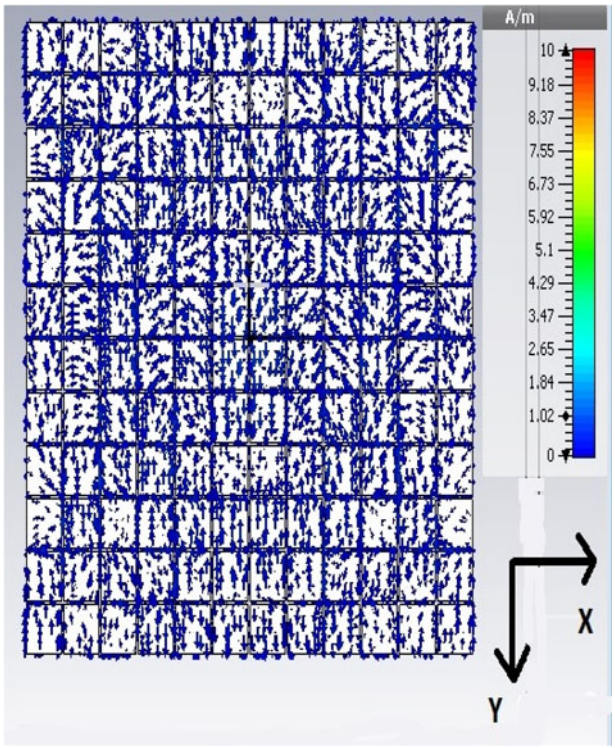

Fig. 8. Simulated current distribution of PRS at 7.78 GHz.

At boresight, the extra directivity in the broadside direction reaches its maximum value [19–21]:

$$D_e = \frac{1+\rho}{1-\rho} \tag{11}$$

and thus high gain can be achieved.

The half-power fractional BW, calculated for a highly reflecting surface with frequency independent reflection characteristics, is [19]

$$BW = \frac{\Delta f}{f_0} = \frac{\lambda}{2\pi L_r}\frac{1-\rho}{\sqrt{\rho}} \tag{12}$$

for getting maximum gain within a certain frequency range the phase of the reflection coefficient of the PRS must satisfy the following relationship: [19]

$$\phi = \frac{4\pi L_r}{c} f - (2N-1)\pi. \tag{13}$$

In our proposed design, the distance L_r optimized such thatequation (13) satisfies and hence realization of the higher gain occurs. Moreover, achievement of high gain can be also explained based on the increase in the total effective aperture area of the antenna. It is observed that, due to PRS, focusing effect becomes dominant. The phase distributions of the radiated fields with a PRS layer is observed to be more uniform than one without the PRS layer, which plays a major role in an increase in effective aperture area and gain. The focusing effect and phase smoothness increases directivity of the antenna and hence gain of the antenna

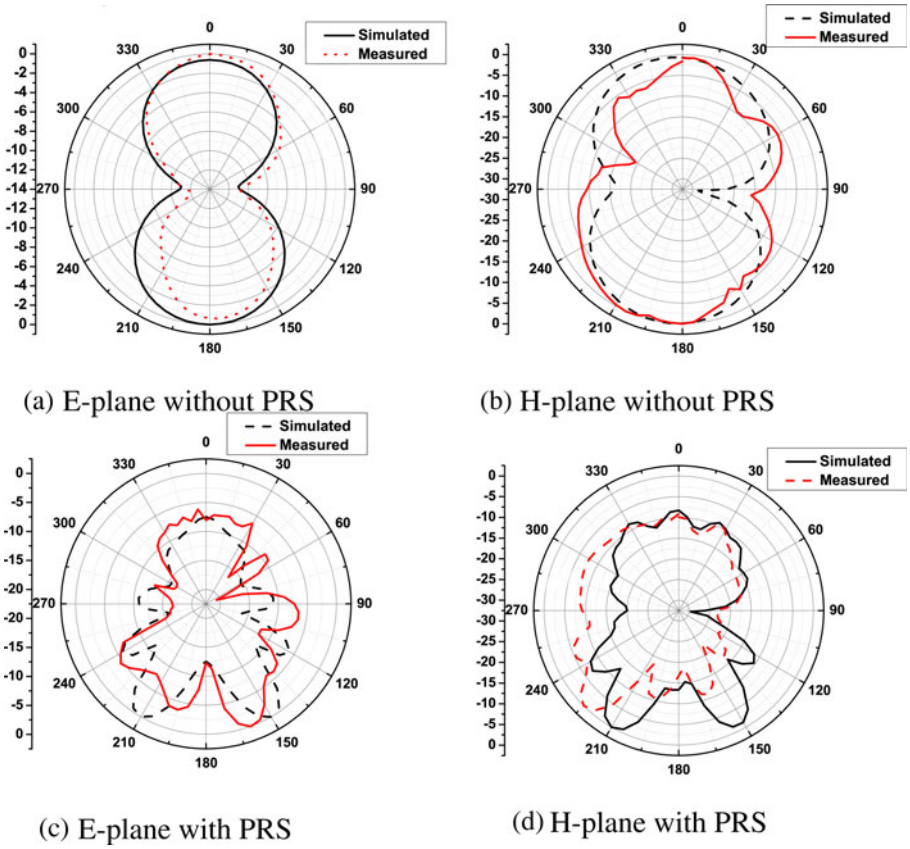

Fig. 9. Simulated and measured radiation patterns of the antenna (with and without PRS). (a) *E*-plane without PRS, (b) *H*-plane without PRS, (c) *E*-plane with PRS, (d) *H*-plane with PRS

https://doi.org/10.1017/S1759078718000326 Published online by Cambridge University Press

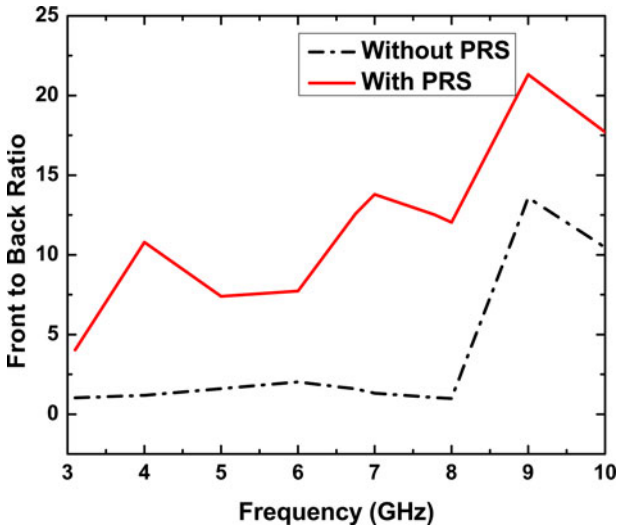

Fig. 10. Comparison of front-to-back ratio of radiation (with and without PRS).

increases. In addition, according to equation (11), the gain of the antenna increases as increment in reflection coefficient [24].

3. Experimental results and discussion

To validate the proposed design, two laboratory prototypes: one without PRS and other one with PRS; were fabricated. The photograph of the both fabricated antennas is shown in Fig. 3. The return loss (S_{11}) of both antennas was measured using 67 GHz Keysight Technologies make (Model no. N5227A PNA) Vector Network Analyzer of Indian Institute of Technology, Roorkee, India; as shown in Fig. 4(a).

The simulated and measured S_{11} of the PRS antenna are given in Fig. 5. In simulation, 3–8.5 GHz BW ($S_{11} \leq -10$ dB) obtained, while in measurement, BW of 3.8–8.8 GHz achieved. The slight mismatch between simulation and measurement of upper and lower cut-off frequencies of BW due to possible tolerance in dielectric constant in substrates, fabrication errors, etc. Here, as per standard definition of useful BW [25], frequency between 3–8.5 GHz considered as useful radiated frequency, eventhough mismatch of the shape of the S_{11}. The simulated frequency response of the antenna gain, which demonstrates the effect of the PRS layer on the gain of the antenna is shown in Fig. 6. It is seen that, when PRS is employed, in the entire frequency band (3–8.5 GHz), average gain increased by 3--4 dB. When CPW fed UWB patch antenna feds SPPA, at boresight high radiation obtained. This is possible only if all PPs are fed in almost same phase and current induces at patches are in the same phase. In our design, all square PPs are embedded at different position of the dielectric layer and have different distance from the radiating element; therefore fed to each square parasitic patch involves different amplitude tapering and phase delay. Because of amplitude tapering, the gain decrease with different frequency. The amplitude tapering increases significantly with the increment in the distance from the radiating element. Thus, the gain of the antenna using PRS depends on PPs dimensions, spacing between two adjacent PPs, resonance distance, etc. [23,24]. The phase delay and amplitude tapering are not so significant between 3 and 4 GHz, hence constant increments in gain obtained between this frequency range, while the same become dominant between 4 and 6 GHz, so gain decrease between this frequency range. Figure 7 shows a gain comparison of simulated and measured results for antenna with and without PRS.

Figure 8 shows the vector current distribution of PRS at 7.78 GHz. The current induced at each square parasitic element is almost in phase and decreases as the distance from the radiating element increases. From the current distribution at PPs, it can be concluded that CPW fed radiating element as well as all PPs contribute to the radiating field. The simulated electric field magnitude distribution for the antenna with and without the PRS, are given in Fig. 11. From this figure, it can be concluded that the electric field

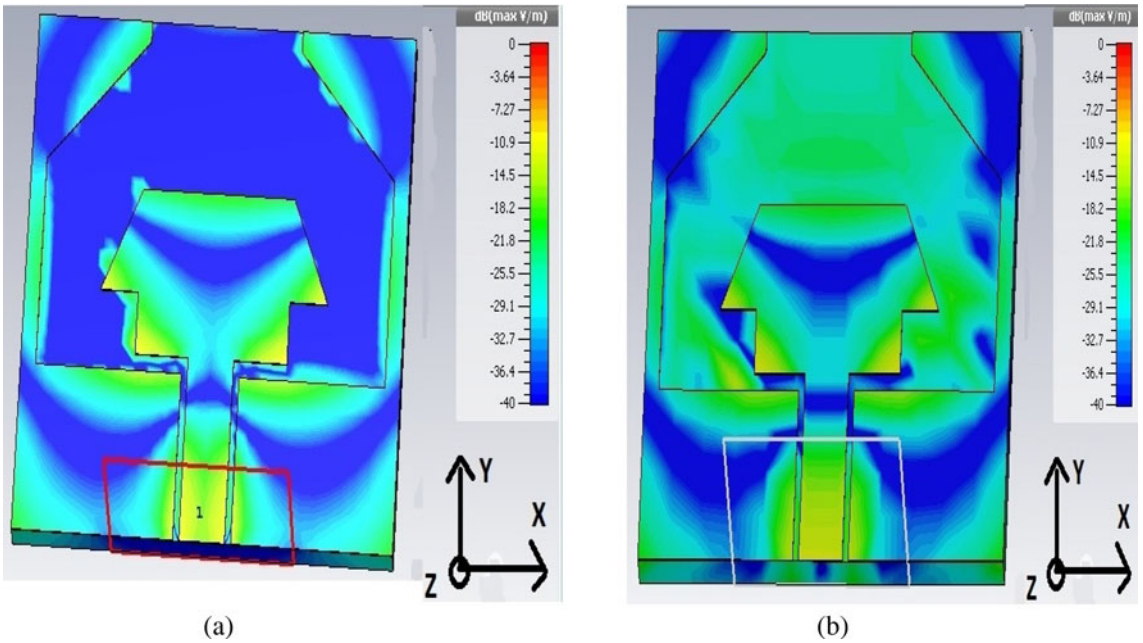

Fig. 11. Electric field magnitude distribution at 7.78 GHz frequency of the antenna: (a) without PRS, (b) with PRS, unit of color bar:dB (Max V/m).

https://doi.org/10.1017/S1759078718000326 Published online by Cambridge University Press

Table 2. Comparison between earlier reported antennas with different gain enhancement techniques and proposed antenna with PRS technique

Ref. no.	Size of antenna (mm^2)	Thickness (mm)	Frequency range	Gain (dB)	Technique used	Gain-Bandwidth product (dB--GHz)
[6]	50 × 50	1.25	530 MHz	4.62 dB conductor layers	Laminated	2.44
[7]	341 × 341	26.8	860–960 MHz	9.7 dBi	Parasitic radiation patch	0.97
[8]	150 × 300	1.9	902–928 MHz	8.7 dBi	Metallic plane	0.22
[9]	11 layers of 60 × 60	66.5	8–9 GHz	7–16.4 dBi	Microwave lens	16.4
[12]	–	2.9	8.9–10.8 GHz	4.02 dB	Zero index Material lens	7.638
[13]	Surface area = 2100	85	1.54 GHz	5.5 dB	High impedance surface	8.47
Our proposed design	Size of PRS = 169 × 169	38.46	3.8–8.8 GHz = 5 GHz	Average 6 dB	PRS	30

distribution of the aperture in case of PRS is more uniform and with higher magnitude as compared with without PRS configuration. Moreover, the effective aperture is also extended by adding the PRS, which leads to achievement of higher gain.

An anechoic chamber was used for measurement of the radiation properties of both the fabricated antennas as shown in Fig. 4(b). The simulated and measured *E* and *H* planes radiation pattern at 7.78 GHz for both configurations (with and without PRS) are shown in Fig. 9. UWB antenna without PRS structure, the main lobe is directed at 175° with 4.81 dB gain with broad half power beam width of 69.8°. Moreover, the side lobe level is −0.5 dB obtained from simulation results, which is very high. The PRS makes the antenna beam highly directive and hence after the introduction of PRS, the main lobe is directed at 150° with 8.53 dB gain with very narrow half-power beam width of 15.3°, which is 219% less than without PRS structure. The side lobe level is −1.5 dB obtained, which is 1 dB less than traditional antenna. Eventhough the main lobe direction will be change at different frequency, but the absolute gain of PRS antenna is higher than without PRS structure. So, it does not affect the application of the antenna. There is no any effect of PRS on the polarization of the antenna. There is good agreement between simulated and measured results.

Due to PRS, the directivity of the antenna increases and back radiation decreases. Figure 10 shows that antenna with PRS gives 3 to 12 time increment of front to back ratio (FBR) as compared to the antenna without PRS.

Table 2 gives comparison of different gain enhancement techniques and proposed antenna with PRS technique. From open literature, we considered the maximum BW and maximum gain obtained using different gain enhancement techniques. Our proposed antenna gives a BW of 3.8--8.8 GHz with a distributed gain of 3.8--8 dB. In the comparative Table 2, for our proposed design, average gain of 6 dB considered. Our proposed antenna gives a maximum gain BW of product of 30 dB--GHz, which is better as compared with reported papers given Table 2.

4. Conclusion

A CPW fed UWB antenna, employed with PRS has been designed and the application of the PRS for the gain enhancement of UWB antenna presented. By properly selecting the resonance distance, the shape of PPs, the space between PPs and optimize their dimensions enhancement of the gain about 3--4 dB obtained in UWB range. The proposed antenna gives rid of poor gain problem in UWB antenna with the cost of increment of size of antenna vertically. By employing uniform incremental/decremental gap spacing between PPs, the phase characteristics of the PRS can be controlled and thus further higher gain can be achieved. This may be the future scope of this work.

Acknowledgments. The author would like to thank the Gujarat Council on Science and Technology, Gandhinagar, Gujarat, India for funding under minor research project program. The authors gratefully acknowledge the department of Indian Institute of Technology, Roorkee, India for providing measurement facility. Authors are also thankful to Charutar Vidyamandal and the management of A D Patel Institute of Technology, Gujarat, India for their inspiration and support.

References

1. **Federal Communications Commission** (2002) Federal Communications Commission Revision of Part 15 of The Commission'S Rules Regarding Ultra-Wideband Transmission System from 3.1 to 10.6 GHz, Washington, DC, USA.
2. **Allen B, Dohler M, Okon E, Malik W, Brown A, Edwards D** (eds). (2007) *Ultrawide Band Antenna and Propagation for Communications, Radar and Imaging*. England: John Wiley & Sons.
3. **Liang XL** (2012) Ultra Wideband Antenna Design: Ultra Widebad Current Status and Future Trends. Chapter 7. InTech Publication.
4. **Gopalkrishna M, Krishna DD, Chandran AR and Anandan CK** (2007) Square monopole antenna for ultra wide band communication applications. *Journal of Electromagnetics Waves and Applications* **21**(11).
5. **Singhal S, Pandey A and Singh A** (2017) CPW-fed circular-shaped fractal antenna with three iterations for UWB applications. *International Journal of Microwave and Wireless Technologies* **9**(2), 373–379.
6. **Ghosh A and Das S** (2014) Gain Enhancement of Slot Antenna Using Laminated Conductor Layers, International Conference on Devices, Circuits and Communications (ICDCCom), Ranchi, India, 1–4.
7. **Zhao X, Huang Y, Li J, Zhang Q and Wen G**, (2017) Wideband High Gain Circularly Polarized UHF RFID Reader Microstrip Antenna And Array. *AEU - International Journal of Electronics and Communications* **77**, 76–81.
8. **Lin YF, Chang MJ, Chen HM and Lai BY** (2016) Gain enhancement of ground radiation antenna for RFID tag mounted on metallic plane. *IEEE Transactions on Antennas and Propagation* **64**(4), 1193–1200.

https://doi.org/10.1017/S1759078718000326 Published online by Cambridge University Press

9. **Cheung SW, Li QL, Wu D, Yuk TI** and (2016) Microwave Lens Using Multi-Layer Substrates For Antenna Gain Enhancement. 10^th European Conference on Antennas and Propagation (EuCAP), Davos, 1–4.
10. **Guan DF, Zhang YS, Qian ZP, Li Y, Cao W and Yuan F** (2016) Compact microstrip patch array antenna with parasitically coupled feed. *IEEE Transactions on Antennas and Propagation* **64**(6), 2531–2534.
11. **Costa F and Monorchio A** (2011) Design of sub-wavelength tunable and steerable fabry-parot leaky wave antennas. *Progress in Electromagnetics Research* **111**, 467–481.
12. **Meng FY, Lyu YL, Zhang K, Wu Q and Li LW** (2012) A detached zero index metamaterial lens for antenna gain enhancement. *Progress In Electromagnetics Research* **132**, 463–478.
13. **Amiri MA, Balanis CA and Birtcher CR** (2017) Gain and bandwidth enhancement of a spiral antenna using a circularly symmetric HIS. *IEEE Antennas and Wireless Propagation Letters* **16**, 1080–1083.
14. **Konstantinidis K, Feresidis P and Hall S** (2014) Multilayer partially reflective surfaces for broadband fabry-perot cavity antennas. *IEEE Transactions on Antennas and Propagation* **62**(7), 3474–3481.
15. **Boutayeb H, Denidni TA and Nedil M** (2007) Bandwidth widening techniques for directive antennas based on partially reflecting surfaces. *Progress in Electromagnetics Research, PIER* **74**, 407–419.
16. **Ge Y, Esselle KP and Bird TS** (2009) Designing A Partially Reflective Surface With Increasing Reflection Phase For Wide-Band EBG Resonator Antennas. IEEE Antennas and Propagation Society International Symposium, Charleston, SC, 1–4.
17. **Pozar D** (1998) *Microwave Engineering*, 2nd edn., New York, NY: Wiley.
18. **CST Microwave Studio Simulator, Version 2017.**
19. **Feresidis AP and Vardaxoglou JC** (2001) High gain planar antenna using optimised partially reflective surfaces. *IEE Proceedings Microwaves, Antennas and Propagation* **148**(6), 345–350.
20. **Tomislav D** (2011) Dynamic Beamwidth Control in Partially Reflective Surface Antennas. PhD Thesis, University of Zagreb, Zagreb.
21. **Khosronejad M and Gentili GG** (2016) Directivity enhancement of a dual-band antenna based on partially reflective surface. 10th European Conference on Antennas and Propagation (EuCAP), Davos, 1–5.
22. **Trentini GV** (1956) Partially reflecting sheet arrays. *IRE Transactions on Antennas and Propagation* **4**, 666–671.
23. **Vaidya AR, Gupta RK, Mishra SK and Mukherjee J** (2012) Efficient high gain with low side lobe level antenna structures using parasitic patches on multilayer superstrate. *Microwave and Optical Technology Letters* **54**(6), 1488–1493.
24. **Vaidya AR, Gupta RK, Mishra SK and Mukherjee J** (2012) High gain low side lobe level fabry parol cavity antenna with feed patch array. *Progress in Electromagnetics Research C* **28**, 223–238.
25. **Balanis CA** (1997) *Antenna Theory Analysis and Design*, 2nd edn., Canada: John Wiley & Sons.

Dr. Pravin R. Prajapati received the B.E. degree from the Government Engineering College, Modasa, Gujarat (1997), and the M.Tech. (Communication Systems) from Indian Institute of Technology, Banaras Hindu University, Varanasi, India (2006). He received his Ph.D. from Indian Institute of Technology, Roorkee, India (2015). Currently, He is working as an Associate Professor of the Department of Electronics and Communication Engineering at A. D. Patel Institute of Technology, Karamsad, Gujarat, India. He is the author/co-author of more than 44 research papers published in the refereed international/national journals and conferences. His research interests include Optical Fiber Communication, RF and Microwave Engineering, Microstrip Antennas, Optical Devices, Power Electronics and Communication Systems. Dr. Prajapati is a member of IEEE Antenna & Wave Propagation Society and life member of ISTE.

Shailesh Khant received his B.E. in Electronics from S. P. University (1997) and Master in Engineering from the same University (2010). Currently he is pursuing his Ph.D. from Charotar University, Changa, Gujarat, India. Currently, He is working as an Assistant Professor at the Department of Electronics and Communication Engineering of A D Patel Institute of Technology, Gujarat, India. His main areas of interest include design of planar antennas, design of advanced Optical Fiber Communication systems, and Microwave Engineering. He is a life member of the ISTE.

https://doi.org/10.1017/S1759078718000326 Published online by Cambridge University Press